34th Annual International Conference of the IEEE EMBS
San Diego, California USA, 28 August - 1 September, 2012

Frequency-Domain Measurement of Neuronal Activity using Dynamic Optical Coherence Tomography

Jonghwan Lee* and David A. Boas, *Member, IEEE*

***Abstract*—We report preliminary results on high-resolution *in vivo* imaging of fast intrinsic optical signals of neuronal activity in the frequency domain. An optical coherence tomography (OCT) system was used for dynamic imaging of the cross section of rodent somatosensory cortex at 250 frame/s. Neurons in the cortex were excited by contralateral forepaw stimulation, and the ipsilateral forepaw was stimulated as a control. Hemodynamic responses at the cortical surface, which were simultaneously measured using a CCD, confirmed that forepaw stimulation properly evoked neuronal activation. Analysis of the OCT signal in the frequency domain resulted in that the spectrum significantly increased at the stimulation frequency during activation. This spectrum change was only observed during contralateral stimulation and highly localized at the stimulation frequency in the frequency space. Therefore, the spectrum change we observed is likely associated with neuronal activation.**

I. Introduction

Spatiotemporal imaging of neuronal activity of the brain plays an important role in the study of brain function and disorders. In particular, an imaging technique based on fast (millisecond scale) intrinsic optical signals (IOSs) will be promising as it has several advantages over conventional techniques: it is noninvasive and label-free; it measures direct neuronal activity, not delayed hemodynamic responses; and potentially it has high-resolution 3D imaging capability enabling us to monitor a large number of positions in parallel.

Optical measurement of neuronal activity has been demonstrated across various levels of the neural system, including isolated nerves [1-4], cultured neurons [5], retinal tissue [6], brain slices [7], exposed cortices [8], and the human brain [9]. However, despite of its potential advantages, 3D *in vivo* imaging of fast IOS has not been realized, mainly due to the small size of the signal (many studies reported $\sim 10^{-4}$ relative changes). The smallness of the signal, especially in *in vivo* measurements, might be oriented from the partial volume effect and/or physiological noise such as the cardiac fluctuation [10-11]. Hence, this study tests the feasibility of depth-resolved *in vivo* imaging of fast IOS by using an optical coherence tomography (OCT) technique that minimizes the partial volume effect and by using frequency-domain analysis that effectively separates physiological noise from the neuronal response. We performed high-speed dynamic OCT imaging of the cross section of the activated region in the somatosensory cortex during forepaw stimulation. This paper presents frequency-domain analysis results including stimulation frequency-specific changes in the spectrum associated with neuronal activation.

This work was supported by the U.S. National Institutes of Health under Grant R01NS057476. *Asterisk indicates corresponding author.*

*J. Lee is with the Martinos Center for Biomedical Imaging, Massachusetts General Hospital, Harvard Medical School, Charlestown, MA 02129 USA (e-mail: jonghwan@nmr.mgh.harvard.edu).

D. A. Boas is with the Martinos Center for Biomedical Imaging, Massachusetts General Hospital, Harvard Medical School, Charlestown, MA 02129 USA (e-mail: dboas@nmr.mgh.harvard.edu).

II. Methods

A. Animal Preparation

Sprague Dawley rats (250-300 g) were initially anesthetized with isofluorane (1.5-2.5%, v/v), and ventilated with a mixture of air and oxygen during surgical procedures. Following tracheotomy and cannulation, the head was fixed in a stereotaxic frame, and the scalp retracted. The skull was thinned over the somatosensory cortex, and the activation region was identified with forepaw stimulation and ball electrode recording. On the activated region, a craniotomy was performed, the dura was carefully removed, and then the brain surface was covered with a glass cover slip. After surgery, rats were anesthetized with a mixture of ketamine-xylazine (20 mg/kg/hr – 2 mg/kg/hr, i.v.). All experimental procedures were approved by the Massachusetts General Hospital Subcommittee on Research Animal Care.

B. Dynamic OCT Imaging of the Cortex

We optimized a spectral-domain optical coherence tomography (SD-OCT) system for dynamic imaging of the rodent cerebral cortex [12]. Based on the result of ball electrode recording, we chose the position for OCT scanning in which the electrical signal was large and there were fewer vessels (Fig. 1A). We acquired dynamic OCT imaging data by repeating B-scans (cross-sectional images consisting of 96 A-scans) at 250 frame/s. The spatial resolution was 3.5 μm (axial) and 7.0 μm (lateral), and the lateral distance between A-scans was 5.0 μm. The intensity image shows the cross-sectional tissue structure (Fig. 1B). An OCT angiogram was obtained by the method reported in the literature [13], showing the cross sections of vessels and their multiple-scattering shadows (Fig. 1C). Simultaneously with OCT imaging, the surface of the cortex was imaged using a CCD and 570-nm wavelength illumination to measure hemodynamic responses. Dynamic CCD imaging was performed at 1.9 frame/s.

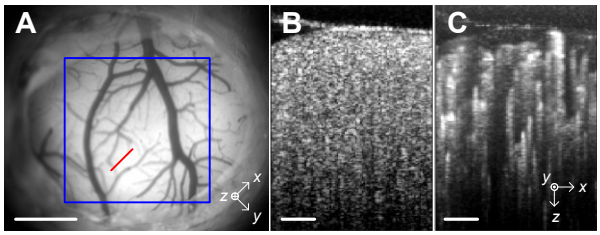

Fig. 1. CCD and OCT imaging of the cortex. (A) A snapshot from dynamic CCD imaging. The red line shows the line of OCT B-scans. The blue box shows the region of interest (ROI) for dynamic CCD imaging analysis in Fig. 3. Scale bar, 1 mm. (B) OCT intensity image in log scale. The magnitude of the OCT signal was averaged over time. Scale bar, 100 μm. (C) OCT angiogram in log scale. Scale bar, 100 μm.

C. Functional Experiment Protocol

While performing dynamic imaging of the somatosensory cortex, we applied electrical stimulation to the forepaw at 3 Hz for 10 s, followed by a 10-s resting period. Each run was repeated ten times for contralateral stimulation, and another ten runs for ipsilateral stimulation. A single animal experiment included five sets of 20 runs at five adjacent Y positions with 20 μm step (Fig. 2).

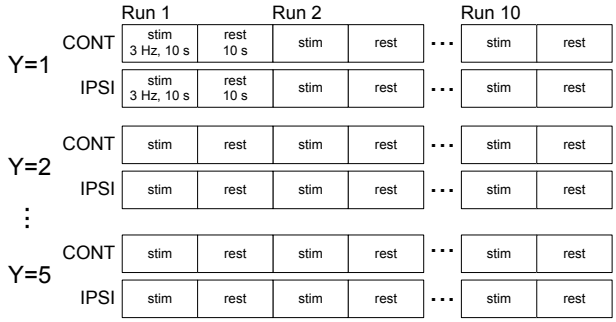

Fig. 2. Functional experiment protocol. Each run consisted of the stimulating period (stim) and the resting period (rest). Ten runs were repeated respectively for contralateral (CONT) and ipsilateral (IPSI) stimulations at five adjacent cross-sectional areas.

D. Data Processing

The functional experiment produced time-domain OCT signals for each Y position:

$$R_{CS/CR/IS/IR}^{(run)}(z,x,t) \qquad (1)$$

where *CS*, *CR*, *IS*, *IR* indicate contralateral stimulation, contralateral resting, ipsilateral stimulation, and ipsilateral resting, respectively. For example, $R_{CS}^{(3)}(z,x,t)$ represents the time-domain signal obtained from the third run of contralateral stimulation. Each signal had 200 x 96 voxels (700 μm x 500 μm) and ~2,500 time points (n_t). The number of time points slightly varied across runs due to the variance in the galvanometer scanning speed, though the variance was smaller than 1%.

Cardiac and respiratory motions of the animal were the primary source of noise in the time-domain OCT signal. The use of the motion correction algorithms that we reported in [12] effectively reduced the motion artifacts. This study used the algorithm removing axial and lateral global phase variations. It improved image stability from 0.5 to 0.8 in terms of the cross-correlation across frames, and reduced phase noise by two orders of magnitude in the stable tissue area.

The motion-corrected signal was Fourier-transformed into the frequency domain, resulting in $R_{CS/CR/IS/IR}^{(run)}(z,x,f)$. Prior to the transformation, the time-domain signal was multiplied by the hamming window to reduce spectral leakage, and then was padded with zeros to increase the sampling rate in the frequency domain. The magnitude of the frequency-domain signal was normalized by $n_t/2$ so that the magnitude at a frequency equals the amplitude of the periodic fluctuation with the frequency in the time-domain signal. The normalized magnitude was squared since the squared magnitude satisfies the energy conservation across domains (Parseval's relation) and thus is more appropriate for the following linear processing (e.g., spatial convolution).

Each spectrum had ~5,000 frequency points with 0.025-Hz resolution. However, the sampling in the frequency domain was slightly different across runs because of the variance in the galvanometer scanning speed. Therefore, the squared magnitude of spectrum was interpolated with the mean frequency sampling prior to averaging across runs. The averaged spectrum was spatially smoothened by being convolved with a 2D Gaussian kernel (15-μm FWHM). Finally, relative changes in the spectrum during stimulation compared to that of the resting period were obtained as in

$$rR_C(z,x,f) = \sqrt{\frac{\left\langle \left| R_{CS}^{(run)}(z,x,f) \right|^2 \right\rangle_{run}}{\left\langle \left| R_{CR}^{(run)}(z,x,f) \right|^2 \right\rangle_{run}}} - 1$$
$$rR_I(z,x,f) = \sqrt{\frac{\left\langle \left| R_{IS}^{(run)}(z,x,f) \right|^2 \right\rangle_{run}}{\left\langle \left| R_{IR}^{(run)}(z,x,f) \right|^2 \right\rangle_{run}}} - 1 \qquad (2)$$

For example, $rR_C(z,x,f) = 0.5$ means that the amplitude of the *f*-Hz fluctuation in the time-domain signal increased by 50% during stimulation compared to the resting period while the stimulation was applied to the contralateral forepaw.

III. Results

A. Hemodynamic Responses Measured by CCD

Data obtained by dynamic CCD imaging were analyzed to visualize hemodynamic responses in the ROI of the cortical surface (blue box in Fig. 1A). The CCD intensity was normalized by the baseline intensity (2 s before the onset of stimulation). Changes in the blood volume were observed during contralateral stimulation, which was significantly larger than those of ipsilateral stimulation (Fig. 3). The hemodynamic response was localized to the bottom half of the ROI. This result confirms that forepaw stimulation excited neurons in the corresponding region of the somatosensory cortex.

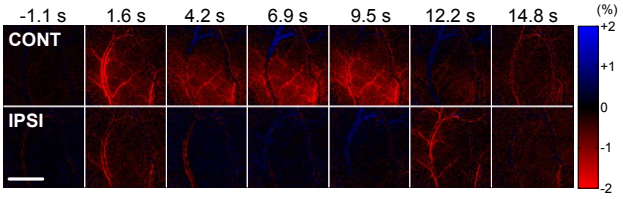

Fig. 3. Dynamic CCD imaging of hemodynamic response. These sequential images present relative changes in the CCD intensity that was averaged across ten runs when OCT was scanning at Y=1. The forepaw was stimulated during 0-10 s. As 570-nm light is mainly absorbed by red blood cells, a decrease in the CCD intensity means an increase in the blood volume. Therefore, red color indicating a decrease in the CCD intensity represents an increase in the blood volume. Scale bar, 1 mm.

B. Spectrum Change at Single Voxel

Fig. 4 shows an example of changes in the spectrum of the OCT signal at a single voxel (the white circle in Y=1 of Fig. 5). The baseline spectrum showed the peak of the respiratory fluctuation (0.9 Hz) and its harmonics, and the peak of the cardiac fluctuation at 6.2 Hz (blue arrows in Fig. 4). Interestingly, the relative change in the spectrum exhibited a peak at the stimulation frequency (3 Hz) during contralateral stimulation (black arrow in Fig. 4). This means that the amplitude of the 3-Hz fluctuation in the time-domain OCT signal at the selected voxel increased 100% when the cortex was activated. The increase in the spectrum was highly localized near 3 Hz in the frequency space, and such a stimulation frequency-specific sharp increase was not observed during ipsilateral stimulation.

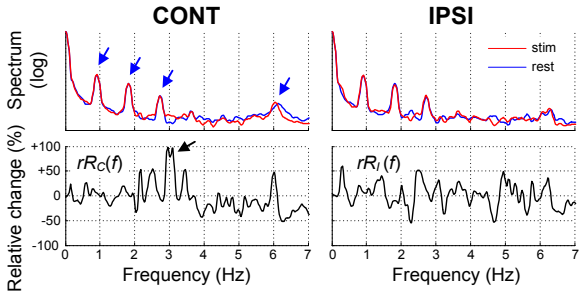

Fig. 4. Spectrum change at the selected voxel. The top row shows each spectrum averaged across runs, for CS (left, red), CR (left, blue), IS (right, red), and IR (right, blue). Relative changes in the spectrum during stimulation, $rR_C(f)$ and $rR_I(f)$, are presented in the bottom row.

C. Cross-sectional Image of Spectrum Change

In order to investigate the spatial distribution of voxels exhibiting stimulation frequency-specific spectrum changes as in Fig. 4, we calculated relative changes in the spectrum for three frequency ranges at every voxel (Eq. 3). The squared magnitude of spectrum was averaged over the given frequencies and across runs before divided by its baseline such that the averaged ratio was not overwhelmed by a single large ratio.

$$rR_C(z,x;f_k) = \sqrt{\frac{\left\langle \int_{f_k} \left| R_{CS}^{(run)}(z,x,f) \right|^2 df \right\rangle_{run}}{\left\langle \int_{f_k} \left| R_{CR}^{(run)}(z,x,f) \right|^2 df \right\rangle_{run}}} - 1$$

$$rR_I(z,x;f_k) = \sqrt{\frac{\left\langle \int_{f_k} \left| R_{IS}^{(run)}(z,x,f) \right|^2 df \right\rangle_{run}}{\left\langle \int_{f_k} \left| R_{IR}^{(run)}(z,x,f) \right|^2 df \right\rangle_{run}}} - 1 \qquad (3)$$

where f_k (k=1,2,3) indicates the three frequency ranges: f_1 = 2.9-3.1 Hz; f_2 = 2.8-2.9 and 3.1-3.2 Hz; and f_3 = 1-5 Hz. These three frequencies were chosen to investigate how much the spectrum change is localized in the frequency space. The first and second frequency ranges were chosen to have the identical size of bin (0.2 Hz).

As a result, a number of voxels exhibited an increase in the spectrum at the stimulation frequency during contralateral stimulation, and the changes were highly localized at 3 Hz in the frequency space (Fig. 5). When we merged five images of the spectrum change via signed-maximum projection in the Y direction, large spectrum changes were only observed at the stimulation frequency and during forepaw stimulation (bottom row in Fig. 5). This result suggests that the observed increase in the 3-Hz fluctuation of the OCT signal is highly associated with neuronal activation.

IV. Discussion and Conclusion

Although the neurophysiological origin underlying fast IOSs has not been entirely resolved, several investigators hypothesized that transient morphological changes in neurons during excitation will cause a change in the optical scattering [3, 7, 14-15]. As the SD-OCT signal is very sensitive to the displacement of scatterers (a 10-nm displacement corresponds to a 0.1 rad phase shift in our system), the morphological change could affect the OCT signal and this response will repeatedly appear every 0.33 s (i.e., at 3 Hz). Even though the amplitude of this response is too small compared to the physiological fluctuations to be seen in the time domain, frequency-domain analysis can effectively separate the neuronal response from the other fluctuations. Furthermore, the probing volume in this study is very small (7 μm x 7 μm x 3.5 μm) such that morphological changes even localized to a part of the soma or neurite bundle may affect the OCT signal with less partial volume effect. These frequency-domain analysis and smallness of the probing volume might enable the measurement of large responses, up to 100% increases in the spectrum amplitude at some voxels. In addition, the cross-sectional architecture of the neuronal response in the merged image exhibited a π-shaped structure, which agrees with knowledge of the pattern of neuronal activity propagation in the somatosensory cortex evoked by forepaw stimulation. It is known that neuronal activation propagates from the deep

layers toward the cortical surface and then spreads in the lateral direction within the superficial layers.

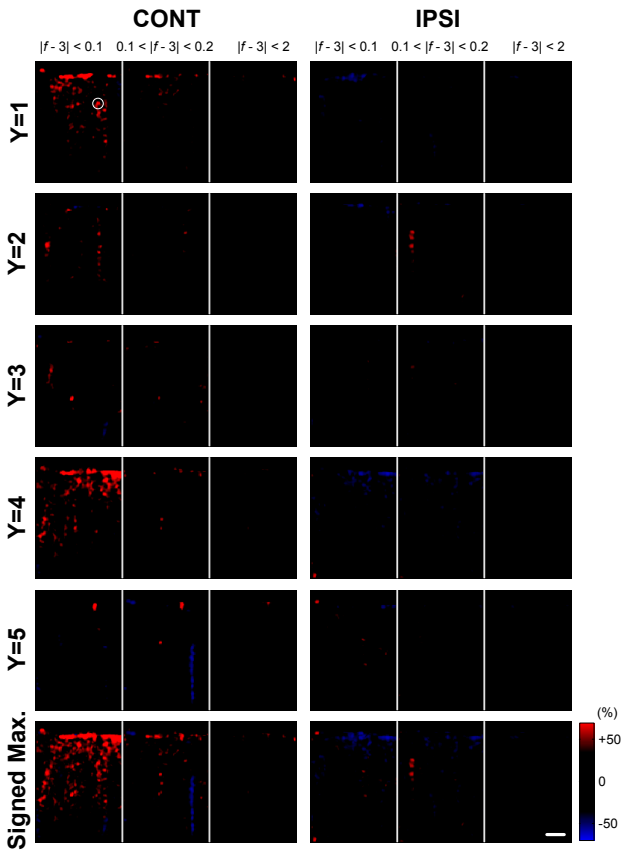

Fig. 5. Cross-sectional image of the spectrum change. Images of relative changes in the spectrum, $rR_C(z,x;f_k)$ and $rR_I(z,x;f_k)$ for three frequency ranges, are presented for each Y position. The bottom row shows the signed-maximum projection of five images along the Y direction. The step between adjacent Y positions was 20 μm. The white circle at Y=1 indicates the voxel selected in Fig. 4. Scale bar, 100 μm.

Another study found that an increase in blood flow responding to neuronal activation in the cortex can cause an increase in the variance of the time-domain OCT signal [16]. Taking into account the Parseval's relation, this suggests the possibility for the hemodynamic response to increase the amplitude of spectrum, which may lead to a result that can look similar to the result presented in this paper. However, as blood flow typically exhibit a slow increase over 1-2 s, the hemodynamics-oriented spectrum change will be global over the frequency space. Therefore, the stimulation frequency-specific spectrum change observed in this study might be attributed to the neuronal response rather than the hemodynamic response. On the other hand, the spectrum change was relatively small in the measurements at Y=2, 3 and 5 (Fig. 5). This result requires further investigation. It is possible that neuronal activation while measuring at the Y positions was relatively smaller due to habituation or physiological instability of the animal. A measurement for each Y position took 10 min involving 600 stimulation trials. We will compare the images of neuronal response shown here to those of hemodynamic response obtained from the same OCT data [16].

Future work will also include validation across animals, as this study presents the result of a single animal; extension to 3D imaging, where we may have to increase the scanning speed; and time-domain analysis. When fully validated, this study will support the feasibility of 3D *in vivo* imaging of fast IOS with micrometer and millisecond resolution. Implementation of the technique will enable label-free live monitoring of the micrometer-scale connectom and thus will be helpful to various types of brain function studies.

REFERENCES

[1] L. B. Cohen, *et al.*, "Light scattering and birefringence changes during nerve activity," *Nature,* vol. 218, pp. 438-41, May 4 1968.

[2] K. M. Carter, *et al.*, "Simultaneous birefringence and scattered light measurements reveal anatomical features in isolated crustacean nerve," *J Neurosci Methods,* vol. 135, pp. 9-16, May 30 2004.

[3] T. Akkin, *et al.*, "Depth-resolved measurement of transient structural changes during action potential propagation," *Biophys J,* vol. 93, pp. 1347-53, Aug 15 2007.

[4] S. Ae Kim, *et al.*, "Optical measurement of neural activity using surface plasmon resonance," *Opt. Lett.,* vol. 33, pp. 914-916, 2008.

[5] R. A. Stepnoski, *et al.*, "Noninvasive detection of changes in membrane potential in cultured neurons by light scattering," *Proc Natl Acad Sci U S A,* vol. 88, pp. 9382-6, Nov 1 1991.

[6] X.-C. Yao and J. S. George, "Dynamic neuroimaging of retinal light responses using fast intrinsic optical signals," *Neuroimage,* vol. 33, pp. 898-906, 2006.

[7] J. Lee and S. J. Kim, "Spectrum measurement of fast optical signal of neural activity in brain tissue and its theoretical origin," *Neuroimage,* vol. 51, pp. 713-22, Jun 2010.

[8] D. M. Rector, *et al.*, "Spatio-temporal mapping of rat whisker barrels with fast scattered light signals," *Neuroimage,* vol. 26, pp. 619-627, 2005.

[9] G. Gratton, *et al.*, "Shades of gray matter: noninvasive optical images of human brain responses during visual stimulation," *Psychophysiology,* vol. 32, pp. 505-9, Sep 1995.

[10] J. Steinbrink, *et al.*, "The fast optical signal--Robust or elusive when non-invasively measured in the human adult?," *Neuroimage,* vol. 26, pp. 996-1008, 2005.

[11] H. Radhakrishnan, *et al.*, "Fast optical signal not detected in awake behaving monkeys," *Neuroimage,* vol. 45, pp. 410-419, 2009.

[12] J. Lee, *et al.*, "Motion correction for phase-resolved dynamic optical coherence tomography imaging of rodent cerebral cortex," *Optics Express,* vol. 19, pp. 21258-21270, 2011.

[13] V. J. Srinivasan, *et al.*, "Rapid volumetric angiography of cortical microvasculature with optical coherence tomography," *Optics Letters,* vol. 35, pp. 43-5, Jan 1 2010.

[14] L. B. Cohen, "Changes in neuron structure during action potential propagation and synaptic transmission," *Physiol Rev,* vol. 53, pp. 373-418, Apr 1973.

[15] J. Lee, *et al.*, "Multiphysics Neuron Model for Cellular Volume Dynamics," *Biomedical Engineering, IEEE Transactions on,* vol. 58, pp. 3000-3003, 2011.

[16] J. Lee, *et al.*, "Depth-resolved imaging of hemodynamic responses using OCT speckle variance analysis," (to be submitted).